INTERNATIONAL JOURNAL FOR NUMERICAL METHODS IN FLUIDS, VOL. 7, 453–464 (1987)

# A STUDY OF THE MOTION IN ROTATING CONTAINERS USING A BOUNDARY FITTED CO-ORDINATE SYSTEM

R. RAGHUNATH AND S. SENGUPTA

*University of Miami Coral Gables, FL 33124, U.S.A.*

AND

J. HAEUSER

*College of Landshut Stethaimerstr. 32-34, 8300 Landshut, West Germany*

## SUMMARY

Numerical solutions are often inaccurate because conventional co-ordinate systems do not represent the complex physical boundaries accurately. In the present work, the numerical solution of linear shallow water wave equations has been obtained by transforming the physical domain into a rectangular computational domain using elliptic differential operators. This work is part of a programme to develop three-dimensional body-fit grid systems for environmental flows. Solutions have been obtained for a cylindrical container and also a parabolic container. The initial conditions chosen are the ones for which analytical solutions exist. The numerical solutions compare well with analytical solutions.

KEY WORDS Boundary Fitted Co-ordinate System Shallow Water Equations Rotating Containers

## INTRODUCTION

The solution of the linear shallow water equations has been of great interest for a very long time. Lord Kelvin, as early as 1880, obtained analytical solutions for oscillations of fluid in a rotating cylindrical container. These solutions may be easily extended to motion in lakes, oceans etc. and are reported in detail by Gray *et al.*[1] and Lamb.[2] Numerical solutions to shallow water equations were obtained by Thacker[3] using irregular grid finite-difference techniques. Thacker[4] has also obtained analytical solutions to non-linear shallow water equations for a parabolic container for certain initial conditions. Haeuser *et al.*[5] have obtained numerical solutions for the linear shallow water equations in a cylindrical ring. The boundary fitted co-ordinate system was used in those solutions.

In the present work, numerical solutions have been obtained for the linear shallow water equations in a cylindrical container and also in a parabolic container. The dimensions of the container are chosen such that the shallow water approximation is valid, and the Coriolis parameter is for a location at a latitude of 26.9° N (e.g. Lake Okeechobee, Florida). The physical domain was transformed into a rectangular computational domain using the transformation methods of Thompson *et al.*[6,7] This transformation helps in the accurate representation of the boundary and accurate application of the boundary conditions. The grid point distribution and the metric coefficients are obtained from the computer codes TOMCAT and FATCAT developed by Thompson *et al.*[7] The governing equation and boundary conditions are also transformed. Although the problems attempted herein have circular boundaries and could have been solved

0271–2091/87/050453–12$06.00


*Received 14 August 1986*
*Revised 16 September 1986*

easily using a polar co-ordinate system, the boundary conforming co-ordinate system has been used to demonstrate the case and accuracy with which solutions may be obtained in the case of irregular domains.

## MATHEMATICAL MODEL

The motion of fluid in a shallow basin is governed by the shallow water wave equations. These equations in the absence of convective terms (low Rossby number) are

*Momentum*

$$\frac{\partial U}{\partial t} - fV + g\frac{\partial h}{\partial x} = 0,$$

$$\frac{\partial V}{\partial t} + fU + g\frac{\partial h}{\partial y} = 0.$$

*Integrated continuity*

$$\frac{\partial h}{\partial t} + \frac{\partial}{\partial x}[U(D+h)] + \frac{\partial}{\partial y}[V(D+h)] = 0$$

In the above equations $U$ and $V$ are the integrated velocities corresponding to the orthogonal directions $x$ and $y$, $h$ is the surface elevation and is positive if it is above the equilibrium level, $D$ is the depth function and is positive below the equilibrium level, $f$ is the Coriolis parameter and accounts for the earth's rotation, and $g$ is the acceleration due to gravity.

The boundary condition used for the solution in the cylindrical domain is that the normal velocity is zero at all solid boundaries. In the case of the parabolic container the velocity gradients are set equal to zero.

Analytical solutions are available for the above set of equations for certain special cases.

## CO-ORDINATE TRANSFORMATION

The governing equations and boundary conditions are transformed from the physical $(x, y)$ co-ordinate system to the transformed system $(\xi, \eta)$. The transformation equations are Laplace equations

$$\xi_{xx} + \xi_{yy} = 0,$$

$$\xi_{xx} + \eta_{yy} = 0,$$

with the boundary conditions

$$\begin{array}{lllll} \xi = \xi_1, & \eta = \eta(x, y) & \text{along} & r = a, & 0 \leqslant \theta \leqslant \pi/2, \\ \xi = \xi(x, y), & \eta = \eta_2 & \text{along} & r = a, & \pi/2 \leqslant \theta \leqslant \pi, \\ \xi = \xi_2, & \eta = \eta(x, y) & \text{along} & r = a, & \pi \leqslant \theta \leqslant 3\pi/2, \\ \xi = \xi(x,y), & \eta = \eta_1 & \text{along} & r = a, & 3\pi/2 \leqslant \theta \leqslant 2\pi. \end{array}$$

The physical domain was fitted with a 109 × 109 grid. The boundary-fitted grid in the physical plane is shown in Figure 1. The complete transformation relations are detailed by Thompson *et al.*[7]

The transformed governing equations and boundary conditions are

*Momentum*

$$\frac{\partial U}{\partial t} - fV + \frac{g}{J}(y_\eta h_\xi - y_\xi h_\eta) = 0,$$

$$\frac{\partial V}{\partial t} - fU + \frac{g}{J}(x_\xi h_\eta - x_\eta h_\xi) = 0.$$

*Continuity*

$$\frac{\partial h}{\partial t} + \frac{1}{J}\{y_\eta[(D+h)U]_\xi - y_\xi[(D+h)U]_\eta\} + \frac{1}{J}\{x_\xi[(D+h)V]_\eta - x_\eta[(D+h)V]_\xi\} = 0.$$

The boundary condition of zero normal velocity is applied by writing the momentum equations in the tangential–normal co-ordinates, imposing the zero normal velocity condition and solving for the tangential velocity. The procedure has been described in detail by Haeuser *et al.*[5] In the numerical solution a staggered grid is used with surface elevation points not present in the boundary. Hence, only the tangential velocity at the boundary is unknown and is obtained by transforming and solving

$$\frac{\partial V_{\hat{t}}}{\partial t} + g\frac{\partial h}{\partial \hat{t}} = 0,$$

where $\hat{t}$ is the tangential co-ordinate.

For the parabolic container the zero velocity gradients boundary condition is applied by equating the $U$ and $V$ velocities at the boundary with the respective velocities at one of the neighbouring points.

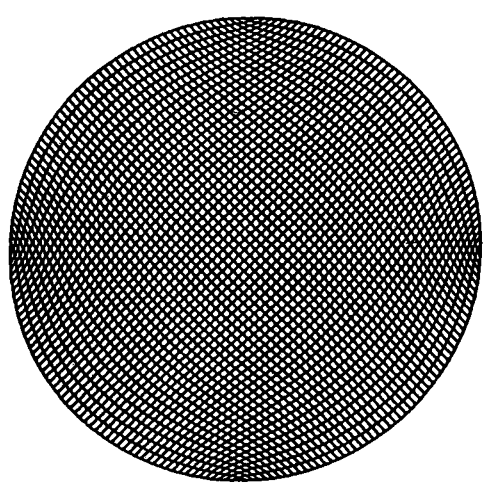

Figure 1. A 55 × 55 boundary-fitted grid in the physical plane

## NUMERICAL PROCEDURE

The transformed equations are approximated by finite difference approximations. A simple, explicit, forward time central space (FTCS) discretization has been used in the present analysis.

The physical domain is first fitted with a boundary fitted co-ordinate mesh, as shown in Figure 1, such that every part of the boundary is either along a $\xi$-line or an $\eta$-line. The co-ordinates and the associated derivatives are obtained using the computer codes TOMCAT and FATCAT developed by Thompson *et al.*[7]

A staggered mesh has been used in the calculation. The velocities $U$ and $V$ are calculated at the full grids and the surface elevation, $h$, is calculated at the half grids. Thus only the tangential velocity is calculated at the boundary points and then resolved into $U$ and $V$ components.

### *Solution algorithm*

1. The initial distribution of the surface elevation and velocities that satisfy the analytical solution are first specified.
2. The tangential velocity, and thus the $U$ and $V$ velocity components at the boundary, are then advanced for the next time step.
3. After that the interior velocities are calculated by solving the momentum equations.
4. The surface elevation is then calculated using the continuity equation.
5. Steps 2–4 are repeated until the desired time.

## RESULTS

### *Analytical*

*Cylindrical container.* For a cylindrical container rotating at angular velocity $\omega$ the general solution is[1]

$$h = J_m(kr)\cos(m\theta - nt),$$

with the boundary condition

$$2m\omega J_m(ka) - nkaJ'_m(ka) = 0,$$

where $a$ is the radius of the container. Also

$$k^2 gD = n^2 - f^2,$$

where $n$ is the angular velocity of oscillation, $f$ is the Coriolis parameter $= 2\omega \sin\phi = 0{\cdot}66 \times 10^{-4}$/s, $\omega$ is the angular velocity of the earth, $\phi$ is the latitude at the point of interest and $D$ is the equilibrium depth of the container.

Figure 2(a) shows the physical domain and the co-ordinate system used. In the present case a container of radius 10,000 m and mean depth 10 m was chosen. The Coriolis parameter was calculated at a latitude of 26·9° N. The mode corresponding to $m = 1$ and the third root of the boundary condition was chosen. For this mode, two nodes are present in the circumferential direction and three in the radial direction.

*Paraboloid.* The analytical solutions of the shallow water equations for a rotating parabolic container have been obtained by Thacker[4] for certain special cases of initial conditions. For the case when the surface is a plane initially, the fluid oscillates such that the surface remains a

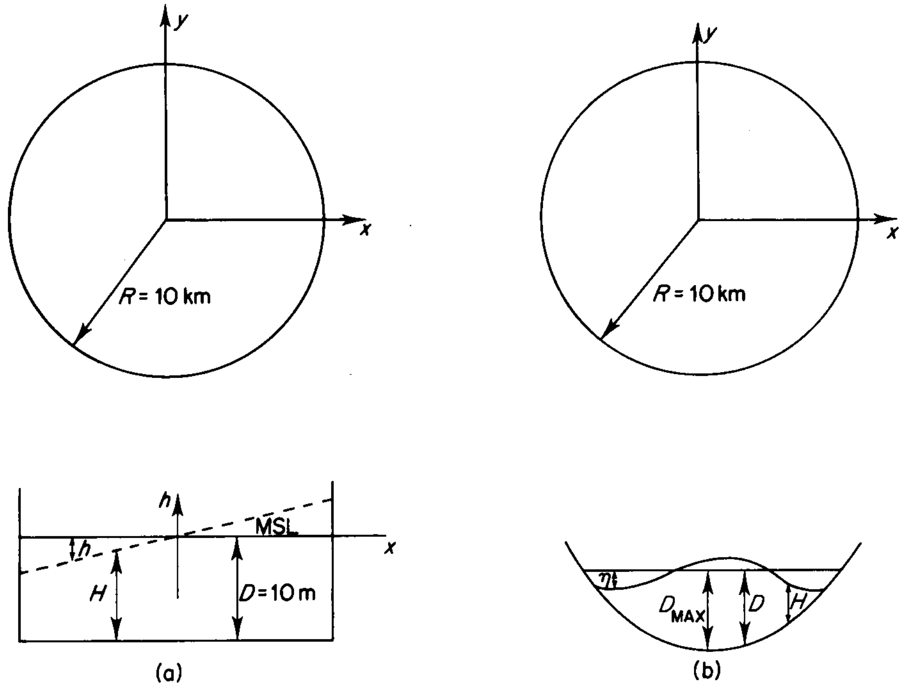


Figure 2. Solution domain in the physical plane and the co-ordinate system: (a) cylindrical domain; (b) parabolic domain $D_{max} = 80$ m

plane and the surface elevation distribution at any given time is

$$h = 2\pi D/L[(x/L)\cos\omega t - (y/L)\sin\omega t - (\eta/2L)]$$

where $\eta$ is related to the amplitude of the oscillation, $L$ is the radius of the container at the equilibrium level, $D$ is the maximum depth and $\omega$ is the angular velocity of oscillation.

A paraboloid of equilibrium level radius 10,000 m and maximum depth 80 m was chosen. The numerical solution is compared with the solution of Thacker.[4] Figure 2(b) shows the physical domain in detail. The amplitude related parameter $\eta$ was set at 50 m and represents the precession of the centre.

*Numerical*

The numerical solution was verified with the exact solutions available. The scheme was tested for stability and convergence for the case of oscillations in a cylinder where the surface elevation is purely a function of the radius. It was found that the analytical stability criterion of $\Delta t \leqslant \Delta X/(\sqrt{2gH})$ was satisfied. The convergence of the scheme was tested for the simplest case of no nodes in the circumferential direction and one node in the radial direction with three different grid sizes. With a $19 \times 19$ mesh the numerical solution had a large error and showed the presence of an artificial mode of oscillation superimposed on the normal mode. The solutions obtained with a $37 \times 37$ mesh and a $55 \times 55$ mesh both agreed very well with the exact solution, suggesting that a $37 \times 37$ mesh was adequate for the resolution of this mode. However, the solutions presented herein are for more complicated cases. The solution in these cases was obtained with three different mesh sizes, 55 × 55, 73 × 73 and 109 × 109, and the solution required the 109 × 109 mesh for good agreement with the exact solution.

*Cylinder*. The mode $m = 1$ was chosen as this allows for nodes in both the radial and circumferential directions. The numerical solution was obtained with a 109 × 109 grid. This yields only a grid of 54 × 54 surface elevation points because of the staggering of the velocity and surface elevation nodes. The surface elevations at a point near the boundary, (1, 1), and at a point in the interior, (26, 26), are shown in Figure 3. Figure 4 shows the $V$-velocity at these

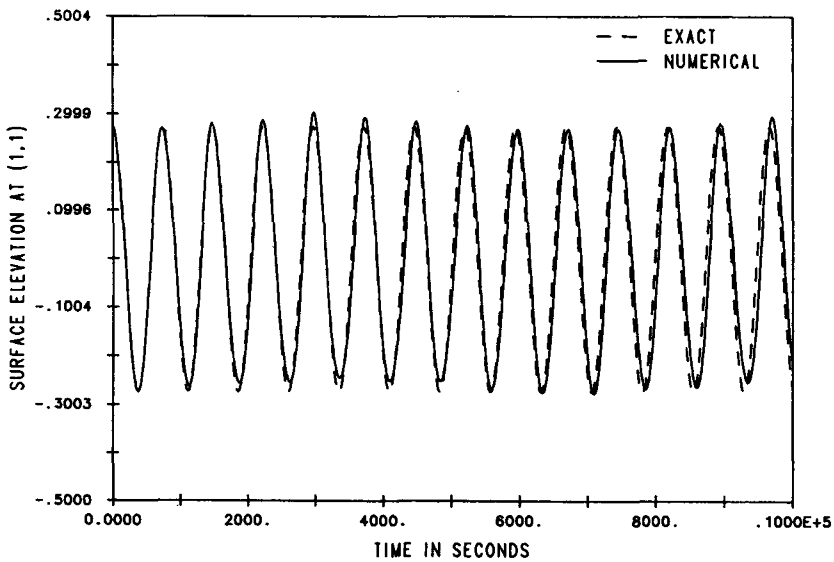


Figure 3(a). Cylindrical container of depth 10 m with a 109 × 109 grid and a time step of 5 s

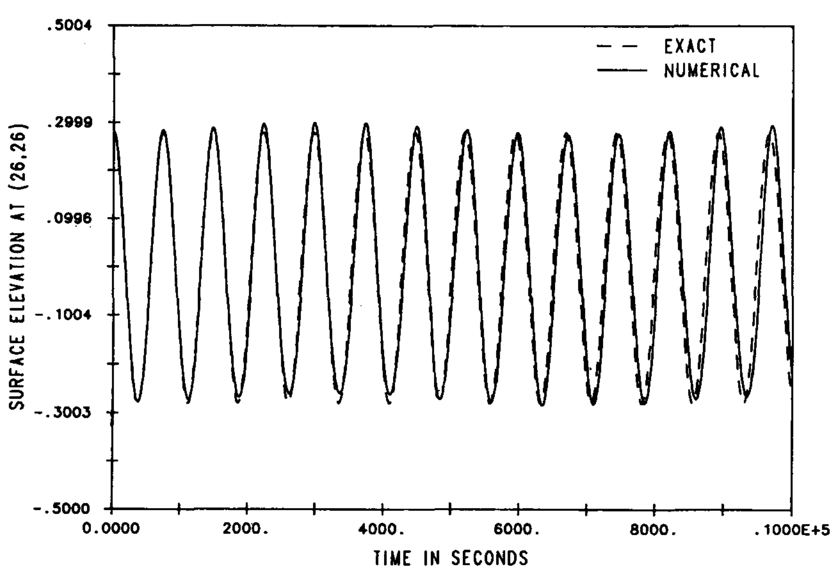


Figure 3(b). Cylindrical container of depth 10 m with a 109 × 109 grid and a time step of 5 s two points. These solutions show that the numerical solution agrees well with the exact solution. During the first five periods the numerical solution shows a slight phase-lead but the amplitude of oscillation matches well with the exact solution. But later both the amplitude and phase are in error. The error in phase grows gradually and the error in amplitude is itself oscillatory. The errors are much smaller in the interior than at the boundaries. Solutions have also been obtained for the lower modes and in these cases the agreement was even better for the same number of grid points. This is anticipated as the accuracy of the numerical solution depends on the number of grid points per wavelength. Three dimensional plots of surface elevation at five different times

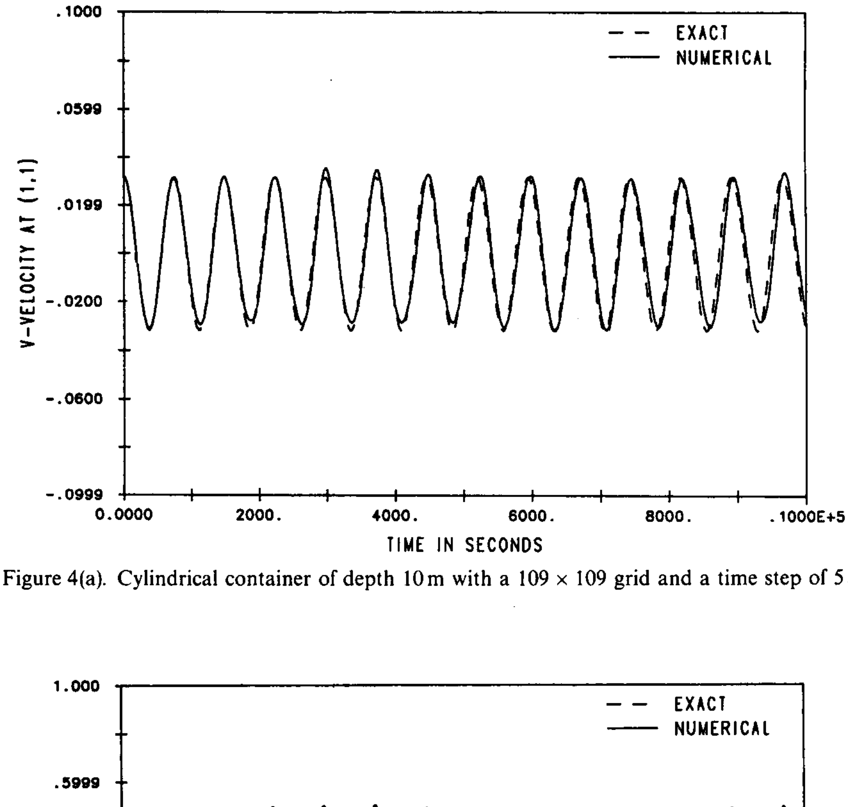


Figure 4(a). Cylindrical container of depth 10 m with a 109 × 109 grid and a time step of 5 s

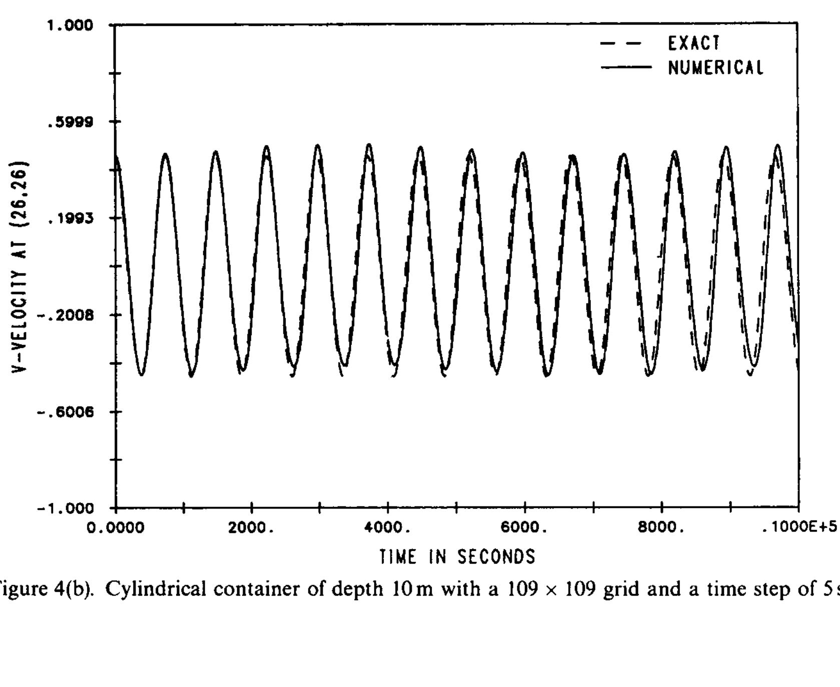


Figure 4(b). Cylindrical container of depth 10 m with a 109 × 109 grid and a time step of 5 s

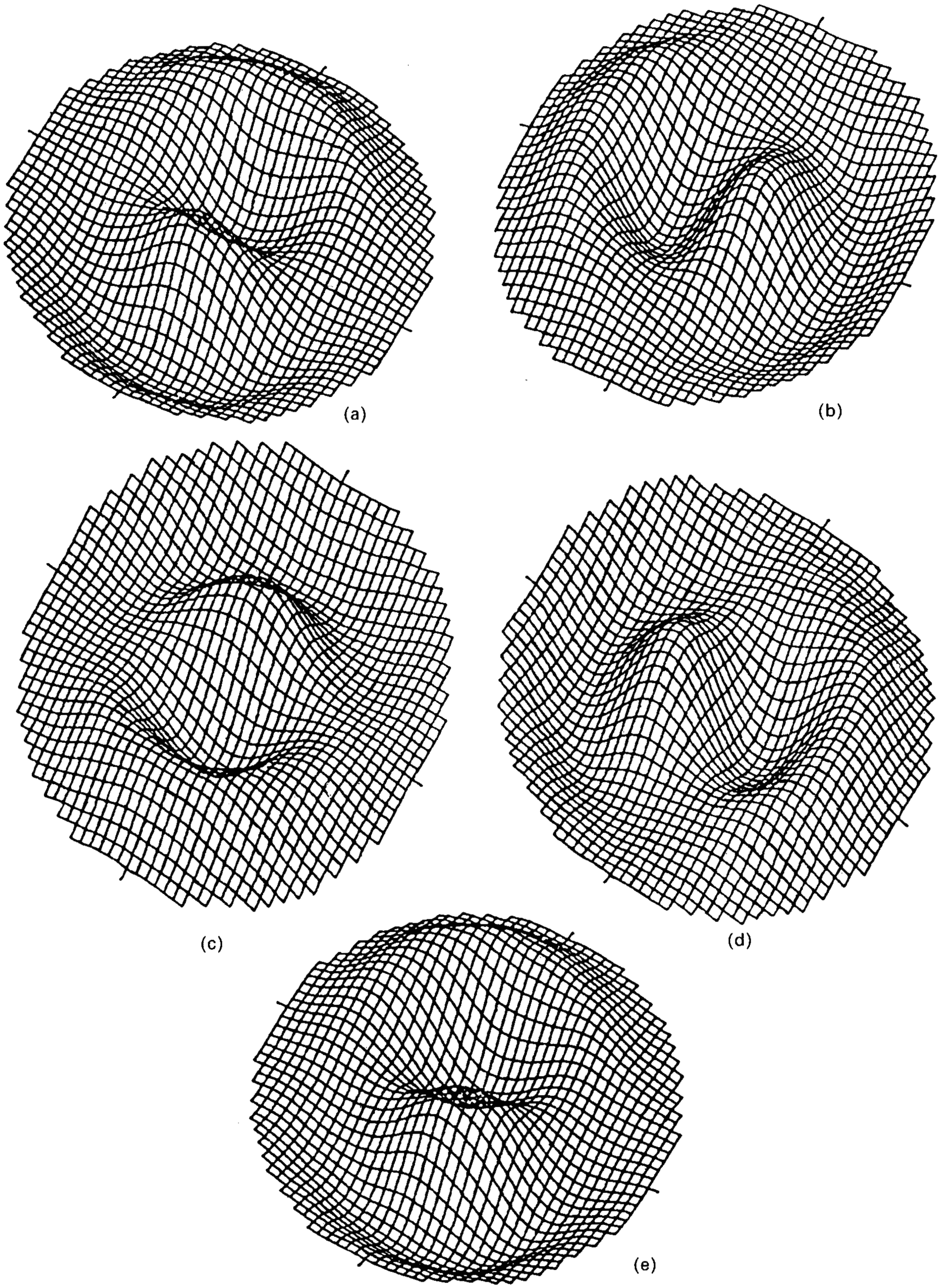


Figure 5. Three-dimensional plot of the surface of fluid in the cylindrical container: (a) $t - 7000$ s; (b) $t - 7200$ s; (c) $t - 7400$ s; (d) $t - 7600$ s; (e) $t - 7800$ s

over a period of oscillation after nearly nine periods are shown in Figure 5. These show clearly that the pattern of solution merely rotates about the centre in a counterclockwise sense with a period close to 800 s.

*Paraboloid.* The solutions for fluid oscillations in a paraboloid are compared with the exact solutions of Thacker.[4] The surface elevation variations with time at two different points in the domain are shown in Figure 6 and the *V*-velocities at these points are shown in Figure 7. These plots show that the numerical solution compares well with the exact solution during the first ten

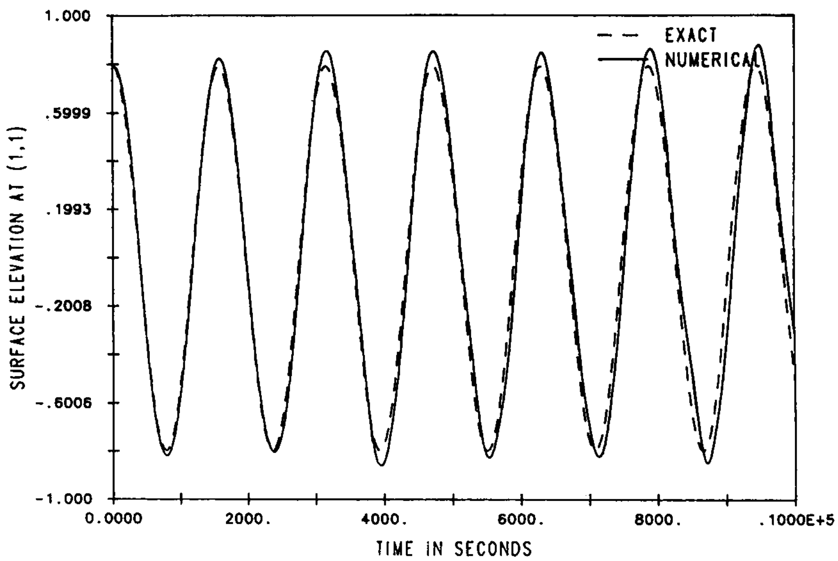


Figure 6(a). Parabolic container of depth 80 m with a 109 × 109 grid and a time step of 5 s

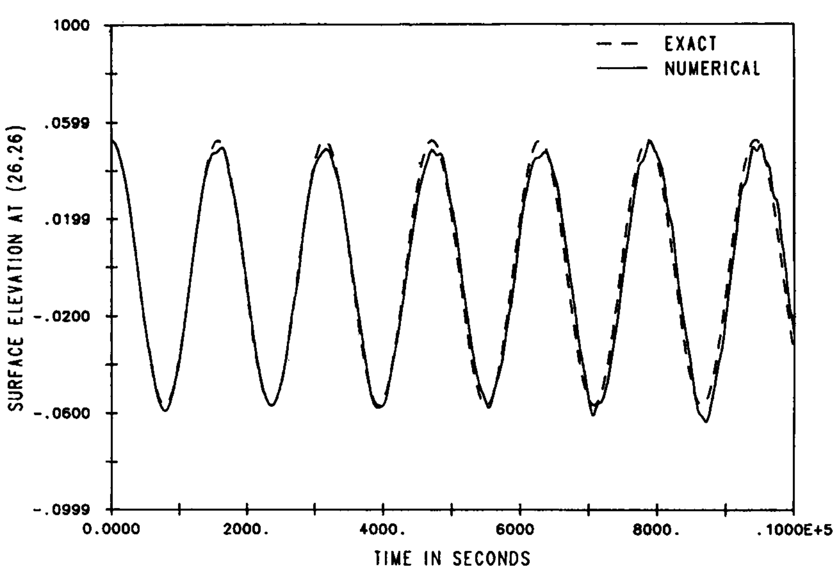


Figure 6(b). Parabolic container of depth 80 m with a 109 × 109 grid and a time step of 5 s

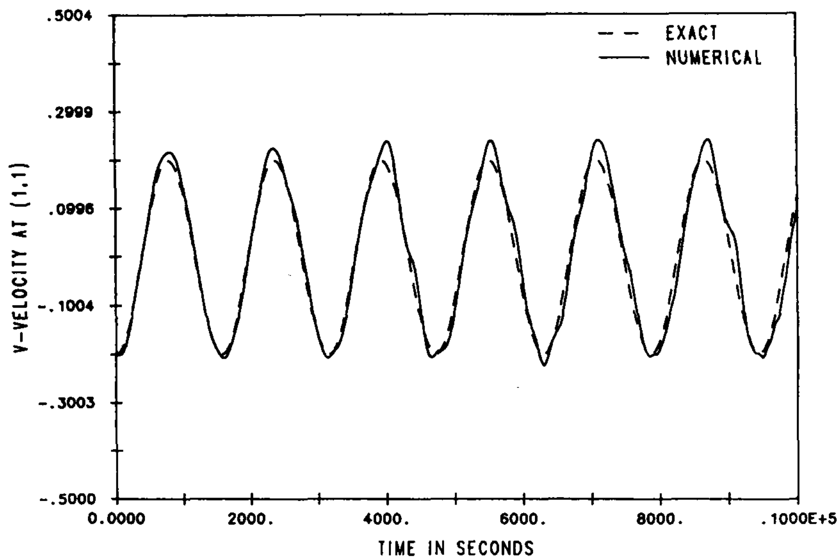


Figure 7(a). Parabolic container of depth 80 m with a 109 × 109 grid and a time step of 5 s

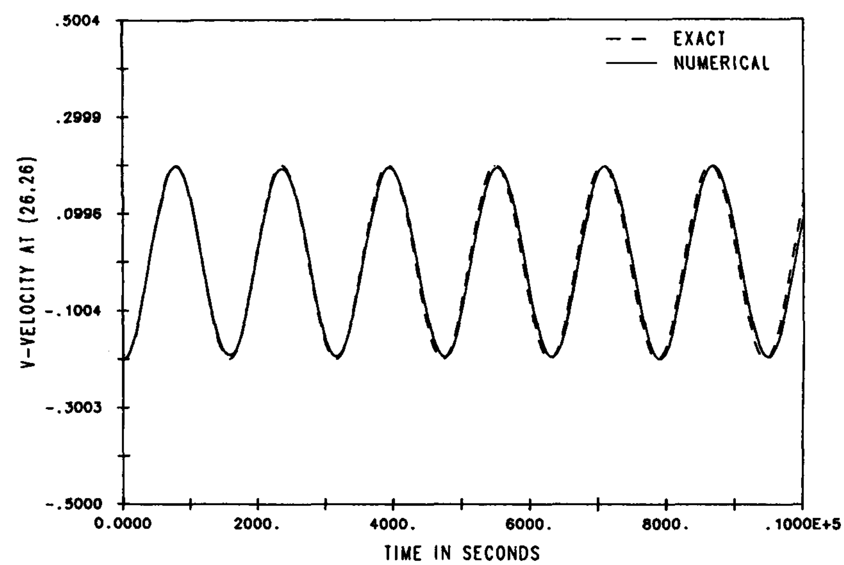


Figure 7(b). Parabolic container of depth 80 m with a 109 × 109 grid and a time step of 5 s

periods. But the solution seems to decay progressively with time. The numerical solution is very well-behaved in the interior initially but slowly the error in the solution at the boundary propagates inside.

The surface is initially a plane and the analytical solution of Thacker[4] dictates that the surface should remain a plane. Contours of surface elevation obtained from the numerical solution after nearly nine periods are shown in Figure 8 for five different times and show the variation over a period. These plots show clearly that the surface remains almost a plane, but close to the boundary there are slight errors.

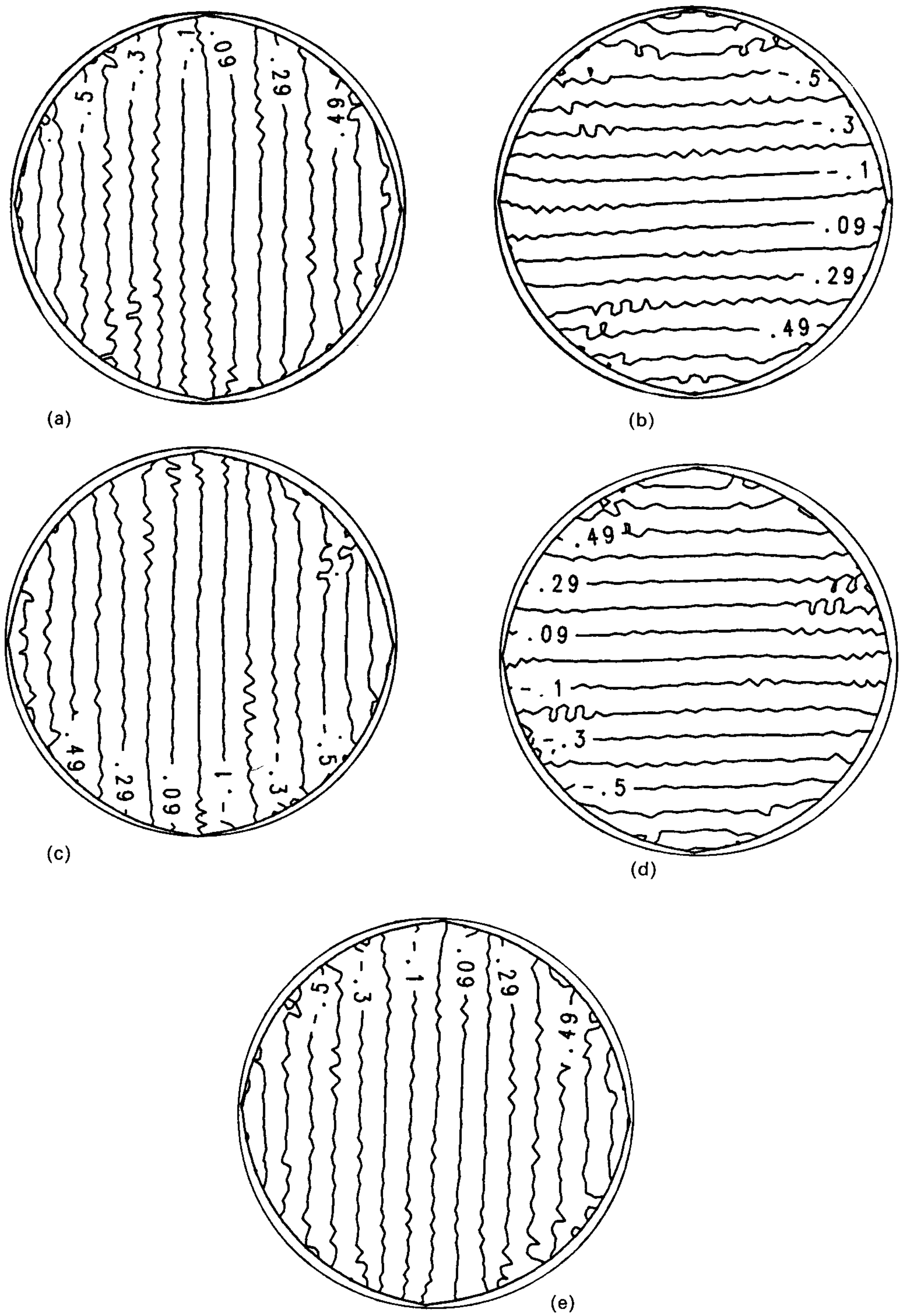


Figure 8. Contours of surface elevation for the parabolic container: (a) $t = 14{,}400$ s; (b) $t = 14{,}800$ s; (c) $t = 15{,}200$ s; (d) $t = 15{,}600$ s; (e) $t = 16{,}000$ s

## DISCUSSION

The cases attempted herein are sufficiently general and show that numerical solutions may just as easily be obtained for arbitrary domains with arbitrary initial conditions. The solution for the cylindrical domain compares well with the exact solution. For the parabolic domain the solution compares well for the first ten periods but there is a slight error at the boundary, probably due to the application of the boundary condition.

These solutions demonstrate that the boundary-fitted co-ordinate system may be used to obtain solutions for the shallow-water equations in irregular domains. The solutions obtained may be made even more accurate with a finer grid.

## ACKNOWLEDGEMENTS

The international co-operation in this work was made possible through a travel grant from NATO 681/84.

## REFERENCES

1. A. Gray and G. B. Mathews, *A Treatise on Bessel Functions and their Applications*, McMillan and Co., Limited, London, 1922.
2. H. Lamb, *Hydrodynamics*, Dover Publications, 1945.
3. W. C. Thacker, 'Irregular grid finite-difference techniques: simulations of oscillations in shallow circular basins', *J. Phys. Oceanogr.*, **7**, 284–292 (1977).
4. W. C. Thacker, 'Some exact solutions to the nonlinear shallow-water wave equations', *J. Fluid Mech.*, **107**, 499–508 (1981).
5. J. Haeuser, H.-G. Paap, D. Eppel and A. Mueller, 'Solution of shallow water equations for complex flow domains via boundary-fitted co-ordinates', *Int. j. numer. methods in Fluids*, **5**, 727–744 (1985).
6. J. F. Thompson, F. C. Thames and W. Mastin, 'Automatic numerical generation of body-fitted curvilinear coordinate system for field containing any number of arbitrary two-dimensional bodies', *J. Comp. Phys.*, **15**, 299–319 (1974).
7. J. F. Thompson, F. C. Thames and W. Mastin, 'Boundary fitted curvilinear coordinate systems for the solution of partial differential equations on fields containing any number of arbitrary two-dimensional bodies', *NASA CR-27292*, 1977.